Space-Dependent Formation of Central Pair Microtubules and Their Interactions with Radial Spokes

Yuki Nakazawa[1¤a], Tetsuro Ariyoshi[1¤b], Akira Noga[1], Ritsu Kamiya[1,2], Masafumi Hirono[1]*

1 Department of Biological Sciences, Graduate School of Science, University of Tokyo, Bunkyo-ku, Tokyo, Japan, 2 Department of Life Science, Faculty of Science, Gakushuin University, Toshima-ku, Tokyo, Japan

Abstract

Cilia and flagella contain nine outer doublet microtubules and a pair of central microtubules. The central pair of microtubules (CP) is important for cilia/flagella beating, as clearly shown by primary ciliary dyskinesia resulting from the loss of the CP. The CP is thought to regulate axonemal dyneins through interaction with radial spokes (RSs). However, the nature of the CP-RS interaction is poorly understood. Here we examine the appearance of CPs in the axonemes of a *Chlamydomonas* mutant, *bld12,* which produces axonemes with 8 to 11 outer-doublets. Most of its 8-doublet axonemes lack CPs. However, in the double mutant of *bld12* and *pf14*, a mutant lacking the RS, most 8-doublet axonemes contain the CP. Thus formation of the CP apparently depends on the internal space limited by the outer doublets and RSs. In 10- or 11-doublet axonemes, only 3–5 RSs are attached to the CP and the doublet arrangement is distorted most likely because the RSs attached to the CP pull the outer doublets toward the axonemal center. The CP orientation in the axonemes varies in double mutants formed between *bld12* and mutants lacking particular CP projections. The mutant *bld12* thus provides the first direct and visual information about the CP-RS interaction, as well as about the mechanism of CP formation.

¤a Current address: Center for Neuroscience, University of California Davis, Davis, California, United States of America
¤b Current address: Department of Neurobiology, Graduate School of Medicine, University of Tokyo, Bunkyo-ku, Tokyo, Japan

Introduction

Motile cilia and flagella are ancient organelles present in various eukaryotic organisms including humans. Defects in structure or motility of cilia and flagella result in a category of diseases called primary ciliary dyskinesia [1,2]. The axoneme of motile cilia and flagella has a strikingly conserved structure consisting of nine outer doublet microtubules and two central-pair (CP) microtubules. These microtubules have various types of projections, such as outer and inner dynein arms, radial spokes (RSs), CP projections and nexin links, which directly or indirectly interact with each other [3–8]. The interactions between these projections must play fundamental roles for maintaining the cylindrical arrangement of the outer doublets, for producing the motive force, and for converting the force to ciliary/flagellar bending waves [9–11]. However, the nature of interaction between these structures is not well understood.

The ninefold symmetrical arrangement of the outer doublets is determined by the centriole (basal body), which has a cylindrical shape consisting of nine short triplet microtubules. Axonemal doublet microtubules assemble onto the A- and B-tubules of each triplet microtubule through a junction called the transition zone [11]. In contrast to the outer doublets assembling on clearly defined template structures, the assembly process of the CP is largely unknown. In *Chlamydomonas* flagella, the distal end of the CP is capped with a plate while the proximal end does not attach to any recognizable structure [12,13]. In *Tetrahymena* cilia, the distal end is also capped with a plate, while the proximal end of one CP microtubule is covered with the axosome, an amorphous structure observed in ciliate axonemes, and the other CP microtubule is apparently associated with no distinct structures [14,15]. Neither of the ends appears to function as the nucleation site for CP assembly [16–20]. However, what nucleates the CP assembly and what determines the CP number in the axoneme are not known.

The CP and RS appear to function as a regulatory system for ciliary and flagellar motility [21–25]. For generation of axonemal beating, a subset of the axonemal dyneins must be activated at a specific phase of beating, and the region of the activated dynein must move along the axoneme as the bending propagates toward the tip. Although the mechanism of this dynein regulation is yet to be elucidated, the CP/RS system clearly plays a crucial role in coordinating dynein activities [9,10,23]. Several lines of evidence suggest that, in some protists including *Chlamydomonas* and *Paramecium*, the CP assumes a twisted conformation and rotates within the axoneme once per beating cycle. The signal of CP orientation is most likely transmitted to the dynein arms through the RS [9,10,26–28]. The CP-RS interaction probably involves mechanical force since the RS is the structure that keeps the CP at the center of the axoneme [24]. In accordance with the probable

mechanical nature of interaction, a recent study has suggested that the RS pushes the CP in beating axonemes [29]. However, the evidence is rather indirect and thus whether the RS pushes or pulls the CP appears to need further studies.

We previously reported a *Chlamydomonas* mutant, *bld12*, that has severe defects in a subcentriolar structure termed the cartwheel [30]. The cartwheel, consisting of a central hub and nine spokes, is located at the proximal end of the centriole as a stack of several layers [31,32]. The mutant *bld12* lacks the central part of the cartwheel due to a null mutation in the gene coding for SAS-6, a component of the cartwheel [30]. X-ray crystallography and biochemical analyses showed that SAS-6 forms a dimer having two globular heads and a coiled coil tail, and the dimers assemble into a ring through their hydrophobic interaction between the heads [33,34].

Lack of the cartwheel in *bld12* causes severe defects in the centriole assembly: ~80% of the centrioles observed are split into fragments and only ~20% are assembled in the cylindrical structure. Interestingly, the number of the triplets varies from seven to eleven in the cylindrical centrioles. As a consequence, flagellar axonemes produced in a small fraction of *bld12* cells contain variable numbers of outer doublet microtubules ranging from eight to eleven [30]. In this study, we investigated the effects of the variation in the outer doublet number on the appearance of the CP within the axoneme. The results revealed the importance of the spatial factor for the formation of the CP, and furthermore, provided evidence for the presence of attractive force between the CP and RS.

Material and Methods

Strains

Chlamydomonas strains CC124 (wild-type), *pf6*, *pf14*, and *pf16* were obtained from the *Chlamydomonas* Resource center, and *cpc1* from Dr. Mitchell of State University of New York Upstate Medical University [35]. The mutant *bld12* (*bld12-1*) was previously isolated in our laboratory (Nakazawa et al., 2007). The double and triple mutants, *bld12pf6*, *bld12pf14*, *bld12pf16*, *bld12cpc1*, *bld12cpc1pf6*, *pf14pf6*, *pf14pf16*, and *pf14cpc1*, were produced by genetic crosses [36]. Cells were grown in Tris-acetate-phosphate (TAP) media [37] with aeration on a 12 h/12 h light/dark cycle, or under constant illumination with agitation.

Preparation of flagellar axonemes

Flagella were isolated from *bld12-1* or *bld12-1cw92* cells by the dibucaine method of Witman [38]. Detached flagella were collected by centrifugation at 10,000×g, overlaid on a sucrose cushion (25% sucrose, 20 mM HEPES pH 7.4) and centrifuged at 1,000×g for 10 min at 4°C. Flagella at the boundary between the upper phase and the sucrose solution was collected, and demembranated by treatment with 0.5% Nonidet P-40 in HMDE solution (30 mM HEPES, 5 mM $MgCl_2$, 1 mM dithiothreitol (DTT), 1 mM EGTA, pH 7.4) [38]. The axonemes collected by centrifugation were resuspended with HMDE solution. For analysis of flagellar length, isolated flagella were collected and their lengths were measured using ImageJ software.

Electron microscopy

Axonemes were prefixed with 2% glutaraldehyde and 1% tannic acids in 50 mM phosphate buffer pH 7.2 for 1–2 h at 0°C, and postfixed with 1% OsO_4 in the phosphate buffer for 1 h. The samples were dehydrated by passing through graded concentrations of alcohol solutions, and embedded in EPON 812. Thin sections (50–70 nm) were stained with aqueous uranyl acetate and Reynold's lead citrate, and observed with a JEM1010 electron microscope. Images were obtained using a film-base camera or MegaView III digital camera (JEOL, Tokhyo). For analysis of axonemal cross sections, images were chosen on the basis of clear appearance of all outer doublets, to ensure that the axoneme under examination was cut almost normal to the axoneme axis. The diameter and inner-doublet spacing were measured using ImageJ software. Correlation between the diameter and the doublet number was analyzed using a linear regression model. Group difference in inter-doublet spacing was analyzed using ANOVA. Statistical significance for the test was set at P<0.05.

Analysis of CP-RS association and helical properties of the CP

For analyses of the CP-RS association, cross section images of 10- or 11-doublet axonemes of *bld12*, *bld12pf6*, *bld12cpc1*, *bld12cpc1pf6*, and *bld12pf16* were chosen and collected based on the clarity of the C1 and C2 microtubules. In the case of *bld12pf16*, images of the 9-doublet axonemes were used for the analysis in addition to the 10- or 11-doublet axonemes. Each image was oriented with the dynein arms projecting clockwise. The CP surface in the image, which was approximated to a circle, was equally divided into 12 sectors. The spokeheads attached to or detached from the CP were identified by visual inspection. The center of the consecutive spokeheads attached to the CP was defined as the spokehead-interaction site. Distribution of the interaction sites on the CP surface was represented by polar histograms.

In the CP orientation analysis in cross section images of *pf14*, *pf14pf6*, *pf14cpc1*, *pf14pf16* axonemes, distribution of the sector closest to the outer doublet wall was represented by polar histograms. Statistical significance of the difference in distribution was evaluated by the χ^2 test. Statistical significance was set at P< 0.05.

Results

Abnormal axonemes in *bld12*

As we previously reported, ~10% of *bld12* cells produced one or two flagella when cell walls were removed by treatment with autolysin [30]. Under this condition, about 8% of cells were uniflagellated and 2% biflagellated. Of the biflagellated cells, about 50% had flagella of unequal lengths. The flagellar length was variable but always shorter than that of wild type (Figure 1A). The *bld12* flagella displayed a variety of motility phenotypes, ranging from complete paralysis to sporadic twitching to almost normal beating.

Electron microscopy showed that the percentage of 8-, 9-, 10-, and 11-doublet axonemes was, respectively, ~5%, ~90%, ~5%, and ~0.1% (Figure 1B) [30]. While the diameter of the axoneme increased with the doublet number, the space between the adjacent doublets was constant (Figure 1C), suggesting that the inter-doublet structures such as the inner- and outer-dynein arms and the nexin links were not distorted in the abnormal axonemes. In the images of these axonemes, we noticed two remarkable features that are not seen in normal axonemes: ~95% of the 8-doublet axonemes had no CP microtubules; and, in 10- or 11-doublet axonemes, the circular arrangement of the doublets was distorted because only three to five RSs were attached to the CP. Similarly distorted axonemes were also observed in intact flagella of this mutant (Yuki Nakazawa, unpublished observation).
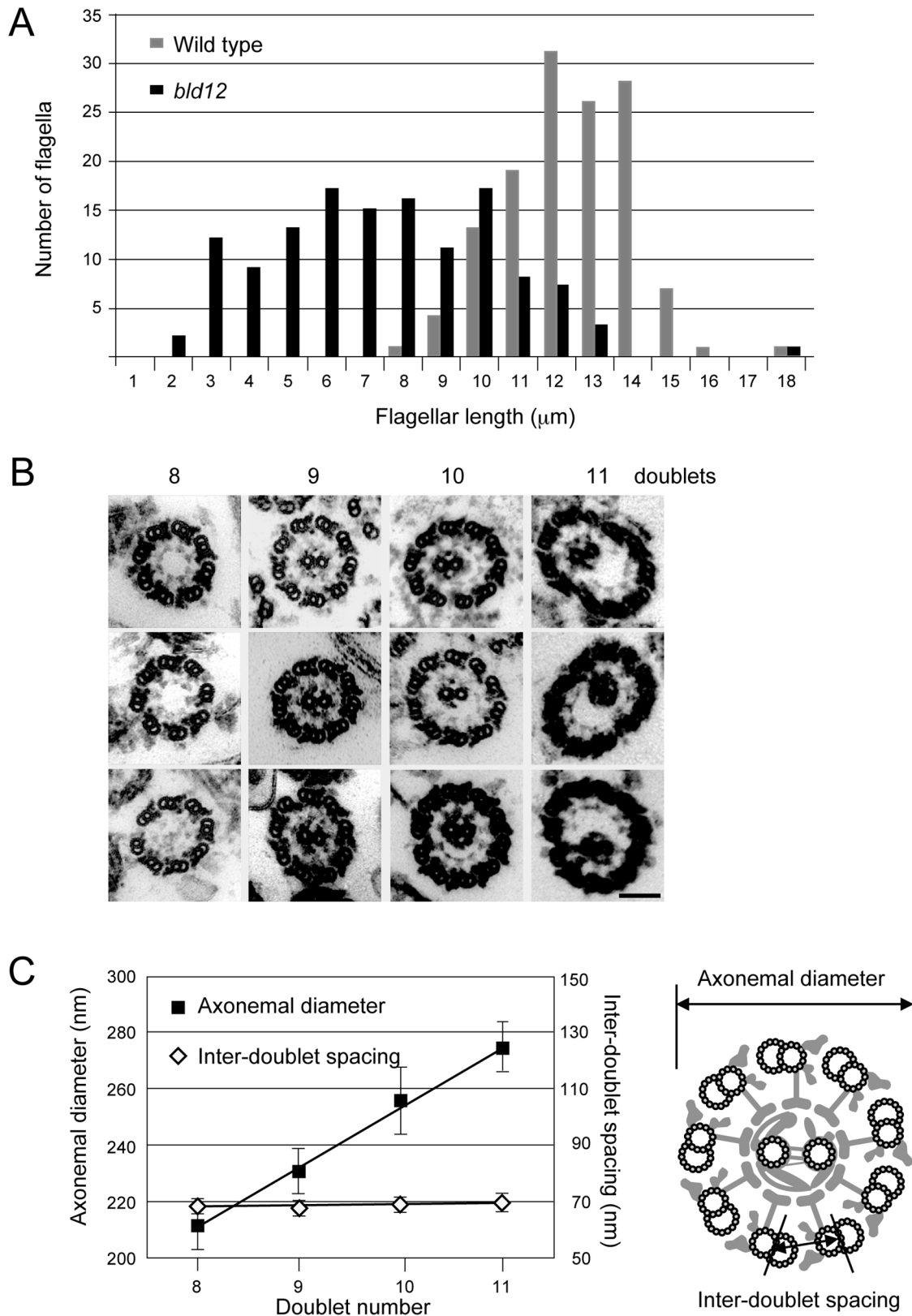
Figure 1. Abnormal features of *bld12* axonemes. (A) Length distributions of wild type (gray) and *bld12* (black) flagella. (B) Axonemes with 8, 9, 10, and 11 outer doublet microtubules. Bar, 100 nm. (C) Diameter and inter-doublet spacing in axonemes with various doublet numbers. Diameter increases with the doublet numbers, while the inter-doublet spacing is constant. The linear regression slope of the diameter is 22.14 ± 1.69 nm ($R^2 = 0.900$). The difference between the inter-doublet spacing is not significant (ANOVA, P = 0.59).
doi:10.1371/journal.pone.0110513.g001

Effects of RS removal on CP formation

Absence of the CP in most of the 8-doublet axonemes led us to assume that these flagella do not have enough room to accommodate a CP in the central area. To test this hypothesis, we produced the double mutant of *bld12* and *pf14*, a mutant that lacks the RSs and has a larger internal space [39]. This mutant, *bld12pf14*, also produced axonemes with a variable number of doublets, ranging from 7 to 11 (Figure 2). As expected, all of the 8-doublet axonemes and even 7-doublet axonemes had the CP (Figure 2, Table 1). In addition, ~5% of the 9-doublet axonemes or ~74% of the 10-doublet axonemes contained three or four central microtubules (Figure 2, Table 1). In *pf14* also, axonemes with three central microtubules were observed although the occurrence was rare (~0.7% in 2000 cross-section images). These observations indicate that the formation of the CP depends on the size of the space limited by the RSs and the outer doublet microtubules.

Spokeheads preferentially bind to distinct sites on the CP surface

Cross section images of the 10- or 11-doublet axonemes of *bld12* showed that five or six doublets were tethered by RSs to the CP to form a semicircle of a normal diameter. The rest of the doublets, not tethered to the CP due to the detachment of RSs, are arranged in another semicircle bulging outward (Figure 1B). Whether an RS was attached or detached could be easily judged from the position of the bulky spokehead. The doublet arrangement was distorted at the junctions of the two semicircles. In contrast, no such distortion was observed in the RS-lacking axonemes of *bld12pf14* (Figure 2). These observations suggest that the RS binds to the CP to help the doublets align in a circular arrangement of a constant diameter, and that the CP-RS binding is strong enough to distort the arrangement in 10- or 11-doublet axonemes.

To investigate whether this RS binding occurs on particular regions on the CP surface, we examined cross-section images of 10- or 11-doublet axonemes for the possible location on the CP where the spokeheads preferentially attach. We divided the CP image in cross section into 12 sectors, and scored the frequency of each sector to locate at the center of the group of CP-associated RSs (Figure 3, A–C). An analysis of 56 cross-section images revealed that the CP surface had two preferred sites for association with the RS: one near the C1a and the other near the C1b projection. These two preferred sites must bind to the spokeheads more strongly than the other regions of the CP.

Previous studies showed that the *Chlamydomonas* CP, when released from the axoneme, forms a helical complex; when contained in the axoneme, it must be forced to assume a straight form with a 360 degree twist per the length of the flagellum [40,41]. This tendency of the CP to assume a helix might bias the distribution of the apparent spoke-interaction sites in the 10- or 11-doublet axonemes (Figure 3, B and C). To address this possibility, we examined the helical tendency of the CP in the spoke-less *pf14* axonemes, in which the CP should assume a small-amplitude helical form facing its outer surface to the outer doublet wall (Figure 3, D and E). An analysis of 80 cross sections of *pf14* axonemes indicated that the C1 microtubule is located outer side of the CP helix, i.e. closest to the doublet wall. This distribution pattern is clearly different from the pattern in the axonemes of *bld12*, which showed two preferred orientation regions (Figure 3, B–E). We therefore concluded that the helical tendency of the CP did not mask the CP orientation resulting from its interaction with RSs.

Removal of CP projections identifies multiple weak CP-spoke association sites

We next examined CP-RS interactions in double mutants between *bld12* and each one of four mutants that lack specific CP projections (Figure 4). The CP mutants used were *pf6* lacking the prominent projection C1a [42]; *cpc1* lacking C1b and C2b [35]; *pf6cpc1* double mutant lacking these three projections; and *pf16* lacking the C1 microtubule [42]. Interestingly, the spokeheads preferentially bound to the C1b–C2b region when the C1a projection was absent, whereas they bound to the C1a–C2a region when C1b and C2b were absent. In *pf6cpc1* or *pf16*, the spokeheads tended to bind to the C1d and C2c regions, or to the C2b region, where binding was only infrequently observed in *bld12* axonemes (Figure 4, A and B). As controls, we also analyzed the axonemal images of double mutants *pf14pf6*, *pf14cpc1*, and *pf14pf16* because we were particularly concerned that the mutant CPs might have varied tendencies to assume helical forms, which might affect the results of our analysis. The histograms obtained in the control experiments showed that the helical tendency was not largely affected by the *pf6*, *cpc1*, or *pf16* mutations (Figure 4C). For example, the *pf14pf16* CP, which lacks the C1 microtubule, displayed the same tendency as the *pf14* CP (Figure 3D); that is, the side of the C2 that would be positioned closest to the C1 in the wild type CP was still positioned on the outside of the helix. These results suggest that, although different regions of the CP surface differ in the spokehead binding affinity, almost the whole area of the CP surface can bind to the spokeheads.

Table 1. The number of axonemes with particular numbers of outer doublets and central microtubules observed in *bld12pf14*.

# of outer doublets per axoneme	# of central microtubules per axoneme		
	0 or 1	2	3 or 4
7	1	2	0
8	0	465	0
9	15	801	42
10	3	5	23
11	0	1	1

(Total number of axonemes counted, 1,369).
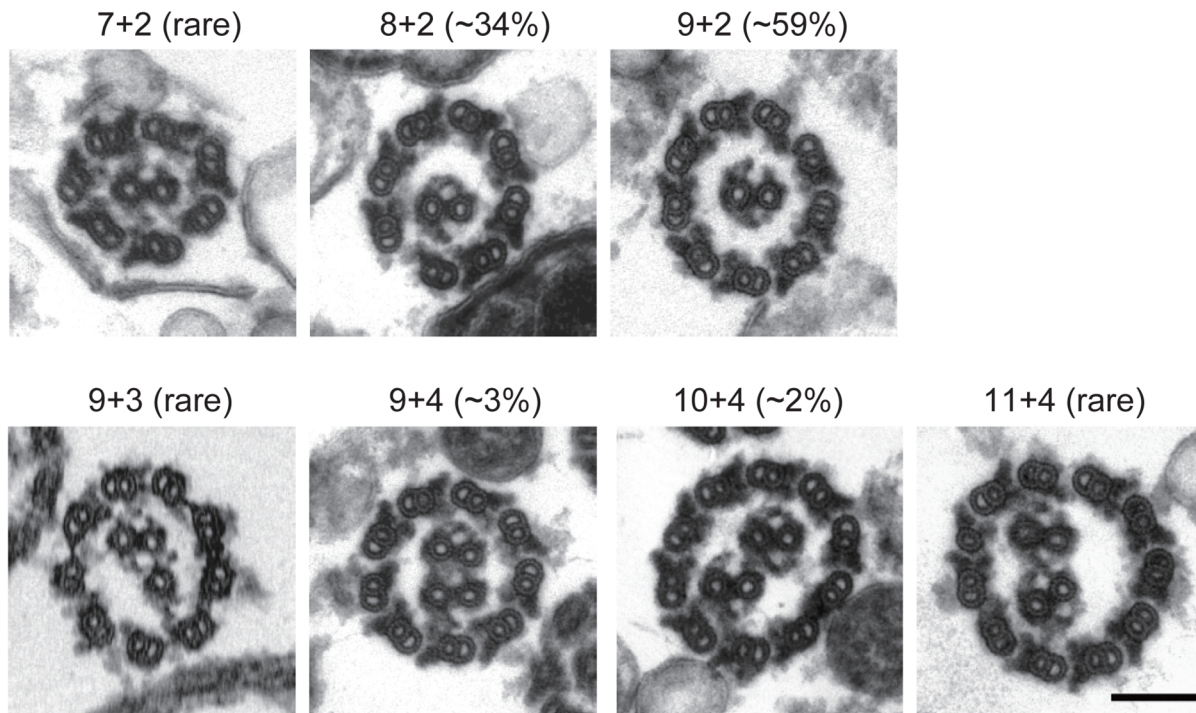doi:10.1371/journal.pone.0110513.t001

Figure 2. CPs in RS-lacking axonemes. Cross section images of *bld12pf14* axonemes with 7 to 10 outer doublets are shown. The frequency of each pattern in the observed images is indicated in the parenthesis (n = 1,369, Table 1). All CPs have the normal polarity in the axoneme as judged by their CP projections. Bar, 100 nm.
doi:10.1371/journal.pone.0110513.g002

Discussion

Formation of the CP

We showed that the CP did not assemble in 8-doublet axonemes of *bld12*, but assembled in those of *bld12pf14* lacking the RS. Furthermore, while 9-doublet axonemes of *bld12pf14* only rarely contained two CPs, its 10-doublet axonemes frequently contained two CPs (Figure 2, Table 1). Formation of two CPs has previously been observed in flagella and cilia that lack the RS: for example, flagella of *Chlamydomonas pf14* and *pf14pf6cpc1* mutants [20,23]; and nodal cilia of rabbit [43]. These observations suggest that CP assembly depends on the internal space of the axoneme. Our results, demonstrating a clear correlation between the CP assembly and the space size, lend strong support to the previous proposal (Table 1).

The distal end of the CP in *Chlamydomonas* flagella and *Tetrahymena* cilia is capped by a plate-like structure that is indirectly attached to the membrane through a spherical bead. In contrast, the proximal end of the CP, located near the transition zone, is associated with no detectable structure [12,13]. In some *Chlamydomonas* mutants with defects in the transition zone, as well as in isolated tracheal epithelial cells, the CP microtubules grow proximally into the centriole, suggesting that the proximal end is not the site of nucleation for CP growth [16,17]. Lechtreck et al. (2013) reported that, when gametes of a *Chlamydomonas* mutant lacking the CP are mated with wild type gametes, the mutant flagella in the fused cells start to produce the CP at the middle portion of the axoneme. This observation indicates that no organizing center is required for the CP assembly at either end of the flagellum. These authors also observed that the RS-lacking *pf14* axonemes contain two CPs (four microtubules) with correct polarity. Together with their findings, our observation of the extra CP in *bld12pf14* implies that the space size within the axoneme is

an important factor that directs CP formation in the axoneme. Possibly, when the CP precursors are present in the axoneme, the CP may form spontaneously without interacting with any template or RSs. In such a case, only the available space and the amount of the precursors may limit the number of the CPs produced.

Nature of CP-RS interaction for the regulation of flagellar motility

A minor population of *bld12* axonemes having 10 or 11 outer doubles exhibited distortion in the circular arrangement of the outer doublets. This observation clearly indicates that the RS binds to the CP and the binding exerts force. Previous studies have provided substantial evidence that the CP and RS form a signal transduction pathway that modulates dynein activity through phosphorylation of a specific subunit of inner-arm dynein [44–46]. The RS is likely to chemically and mechanically control the dynein activity based on the interaction between the CP projections and the spokeheads [9,21]. However, whether or not the RS exerts mechanical force on the outer doublet has been unknown. Our present study is the first to show that RSs actually pull the outer doublet microtubules toward the axonemal center. Such a mechanical force may be at the center of the regulatory function of the CP/RS.

The CP-RS interaction should be transient and the binding strength is weak enough to allow such an interaction. This is because the *Chlamydomonas* CP rotates within the axoneme [40,41] and the RS slides over the CP for a certain distance as the axoneme propagates bending waves [47]. In this study, however, we showed that the interaction is still strong enough to distort the circular arrangement of the outer doublets. This finding prompts us to speculate that the mechanical force transmitted by the RS could change the relative position of the doublet microtubules and
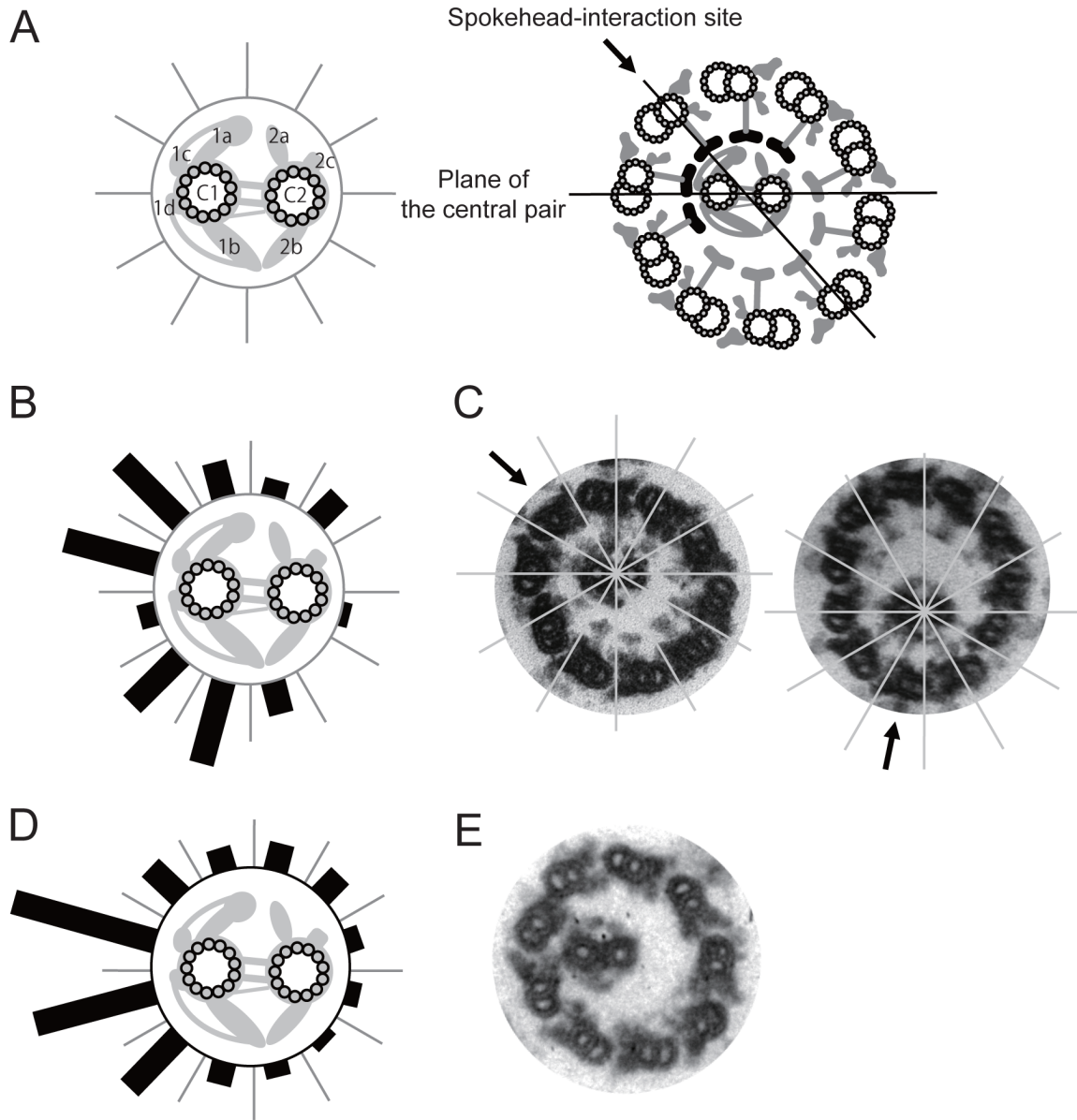
Figure 3. Frequency of CP-RS association in different sectors of the CPs. (A) The CP cross section was divided into 12 sectors by six lines including the one connecting the centers of the two central microtubules. The center of the consecutive spokeheads in contact with the CP was defined as the spokehead-interaction site. Major CP projections are designated [35]. (B) A polar histogram representing the distribution of the spokehead-interaction sites on the CP in cross section images of 10- or 11-doublet axonemes of *bld12* (n = 56). The length of each bar represents relative frequency to locate at the spokehead-interaction site. (C) Axoneme images that correspond to the two peaks in the histogram in (B). (D) Distribution of the CP region in contact with the wall of outer doublets in *pf14* axonemes (n = 80). The histogram suggests that the C1 microtubule is located on the outer surface on the helical CP. (E) A cross section image that represents the peak distribution in the histogram in (D). The differences between the distributions of *bld12* (B) and *pf14* (D) are significant (χ^2 test, p<0.05).
doi:10.1371/journal.pone.0110513.g003

dyneins, and thereby transiently activate or inactivate the dyneins located in a particular region of the axoneme. A change in the dynein-microtubule positioning has also been postulated in the geometric clutch model of Lindemann [48]. The location of dynein molecules activated or inactivated by the CP/RS should propagate along the axoneme as the twisted CP rotates. In the cilia and flagella of multicellular organisms and some unicellular organisms, the CP neither assumes a helical shape nor rotates in the axoneme although sharing the structure and components with the *Chlamydomonas* CP [23,49,50]; in those organisms, the stationary CP determines the plane of axonemal beating possibly

by activating dynein molecules on a particular side of the axoneme [51,52].

Our image analyses of mutant axonemes suggest that, while most area of the CP surface can bind to the RS, the two major projections on the C1 microtubule bind stronger than the other projections on the C2 microtubule. This asymmetric distribution of the RS binding affinities on the CP surface must be important for the signal generation by the rotating CP. Although the present study does not provide information as to whether the stronger binding promotes or inhibits dynein-driven microtubule sliding, previous studies suggest that the C1 microtubule or its projections
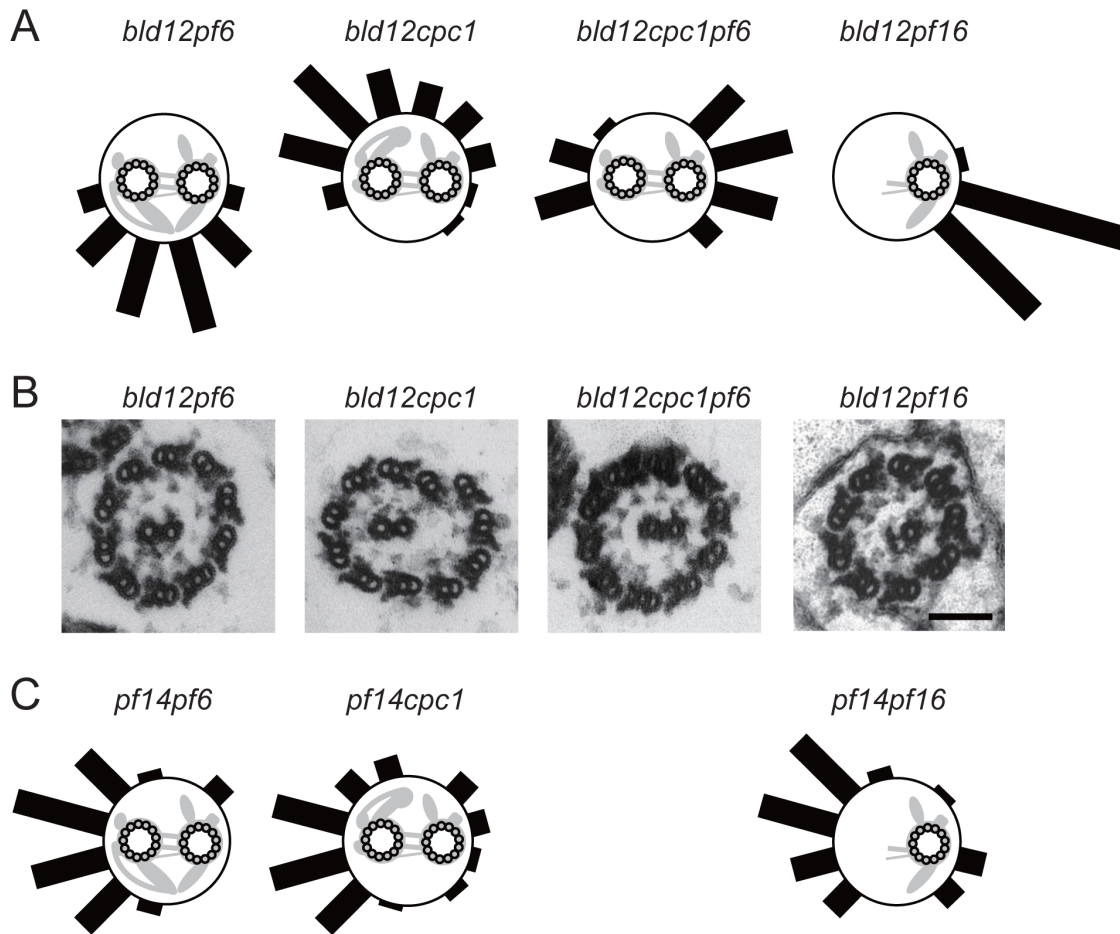
Figure 4. Removal of CP projections manifests weak CP-spokehead association. (A) Distributions of the spokehead-interaction sites on the CP in cross section images of 10- or 11-doublet axonemes of *bld12pf6*, *bld12cpc1*, *bld12cpc1pf6*, and *bld12pf16* (n = 59, 49, 40, and 41), which lack specific CP projections. (B) Cross section images that represent the peaks in the histograms in (A). (C) Distributions of contact sites on the CP surface with the outer doublet wall in cross section images of *pf14pf6*, *pf14cpc1*, and *pf14pf16* (n = 33, 69, and 46). The differences between the distributions of *bld12pf6* and *pf14pf6*; between *bld12cpc1* and *pf14cpc1*, and between *bld12pf16* and *pf14pf16*, are significant (χ^2 test, p<0.05 for each of the three pairs). These distribution patterns are similar to the pattern in *pf14*.
doi:10.1371/journal.pone.0110513.g004

enhances microtubule sliding in axonemes [46,53–55]. Thus the doublet-pulling by stronger RS binding to the C1 surface may activate dyneins and promote microtubule sliding.

Our results are in apparent contradiction with a non-specific CP-RS interaction model recently proposed by Oda et al. (2014). These authors showed that the flagella of the *pf6* mutant lacking the C1a projection recovered motility if any one of three protein tags (hemagglutinin, biotin carboxyl carrier protein, and green fluorescent protein) was attached on top of the spokehead. Because the extent of motility recovery increased in the order of the size of the tag, they proposed that the added tag elongated the RS and compensated the loss of the C1a projection, possibly by enabling RSs to collide with the CP. The proposed physical CP-RS interaction must be non-specific since the three protein tags used are structurally unrelated. In contrast, our analysis of 10- or 11-doublet axoneme images showed that the C1a projection, together with the C1b projection, preferentially associates with the RSs among all the CP projections, favoring the view that the C1a projection pulls the outer doublet in a fairly specific manner. Both their results and our results must reflect some aspects of the CP-RS interaction, but their relationship is not understood. The

molecular mechanism of the CP-RS interaction remains one of the most interesting problems in cilia/flagella motility studies.

An obvious question regarding the present study is whether or not the axonemes with aberrant numbers of outer doublets are motile. We may imagine that 8-doublet flagella are non-motile because they lack the CP, like the flagella of non-motile mutants such as *pf18* and *pf19* [56–58]. However, it is difficult to predict whether or not axonemes with 10 or 11 doublets can display some motility. Development of techniques that determine the number of axonemal microtubules under the microscope, or those that permit constant production of flagella with 10–11 doublets, may well provide answers. We can hope that the answer will provide a strong clue as to why motile cilia and flagella almost always contain nine outer doublets.

Acknowledgments

Author Contributions

References

1. Badano JL, Mitsuma N, Beales PL, Katsanis N (2006) The ciliopathies: an emerging class of human genetic disorders. Annual review of genomics and human genetics 7: 125–148.
2. Onoufriadis A, Shoemark A, Schmidts M, Patel M, Jimenez G, et al. (2014) Targeted NGS gene panel identifies mutations in RSPH1 causing primary ciliary dyskinesia and a common mechanism for ciliary central pair agenesis due to radial spoke defects. Human molecular genetics 23: 3362–3374.
3. Bui KH, Yagi T, Yamamoto R, Kamiya R, Ishikawa T (2012) Polarity and asymmetry in the arrangement of dynein and related structures in the Chlamydomonas axoneme. The Journal of cell biology 198: 913–925.
4. Bui KH, Sakakibara H, Movassagh T, Oiwa K, Ishikawa T (2008) Molecular architecture of inner dynein arms in situ in Chlamydomonas reinhardtii flagella. The Journal of cell biology 183: 923–932.
5. Pigino G, Bui KH, Maheshwari A, Lupetti P, Diener D, et al. (2011) Cryoelectron tomography of radial spokes in cilia and flagella. The Journal of cell biology 195: 673–687.
6. Nicastro D, Schwartz C, Pierson J, Gaudette R, Porter ME, et al. (2006) The molecular architecture of axonemes revealed by cryoelectron tomography. Science 313: 944–948.
7. Heuser T, Raytchev M, Krell J, Porter ME, Nicastro D (2009) The dynein regulatory complex is the nexin link and a major regulatory node in cilia and flagella. The Journal of cell biology 187: 921–933.
8. Carbajal-Gonzalez BI, Heuser T, Fu X, Lin J, Smith BW, et al. (2013) Conserved structural motifs in the central pair complex of eukaryotic flagella. Cytoskeleton (Hoboken, NJ) 70: 101–120.
9. Smith EF, Yang P (2004) The radial spokes and central apparatus: mechano-chemical transducers that regulate flagellar motility. Cell motility and the cytoskeleton 57: 8–17.
10. Kamiya R (2002) Functional diversity of axonemal dyneins as studied in Chlamydomonas mutants. International review of cytology 219: 115–155.
11. Mizuno N, Taschner M, Engel BD, Lorentzen E (2012) Structural studies of ciliary components. Journal of molecular biology 422: 163–180.
12. Dentler WL, Rosenbaum JL (1977) Flagellar elongation and shortening in Chlamydomonas. III. structures attached to the tips of flagellar microtubules and their relationship to the directionality of flagellar microtubule assembly. The Journal of cell biology 74: 747–759.
13. Dentler WL (1980) Structures linking the tips of ciliary and flagellar microtubules to the membrane. Journal of cell science 42: 207–220.
14. Allen RD (1969) The morphogenesis of basal bodies and accessory structures of the cortex of the ciliated protozoan Tetrahymena pyriformis. The Journal of cell biology 40: 716–733.
15. Dute R, Kung C (1978) Ultrastructure of the proximal region of somatic cilia in Paramecium tetraurelia. The Journal of cell biology 78: 451–464.
16. Dentler WL, LeCluyse EL (1982) The effects of structures attached to the tips of tracheal ciliary microtubules on the nucleation of microtubule assembly in vitro. Progress in clinical and biological research 80: 13–18.
17. Jarvik JW, Suhan JP (1991) The role of the flagellar transition region: Inferences from the analysis of a Chlamydomonas mutant with defective transition region structures. Journal of cell science 99: 731–740.
18. Silflow CD, Liu B, LaVoie M, Richardson EA, Palevitz BA (1999) Gamma-tubulin in Chlamydomonas: characterization of the gene and localization of the gene product in cells. Cell motility and the cytoskeleton 42: 285–297.
19. McKean PG, Baines A, Vaughan S, Gull K (2003) Gamma-tubulin functions in the nucleation of a discrete subset of microtubules in the eukaryotic flagellum. Current biology: CB 13: 598–602.
20. Lechtreck KF, Gould TJ, Witman GB (2013) Flagellar central pair assembly in Chlamydomonas reinhardtii. Cilia 2: 15.
21. Wirschell M, Nicastro D, Porter ME, Sale WS (2009) Chapter 9 - The Regulation of Axonemal Bending. In: Harris EH, Stern DB, Witman GB, editors. The Chlamydomonas Sourcebook (Second Edition). London: Academic Press. 253–282.
22. Yang P, Smith EF (2009) Chapter 7 - The Flagellar Radial Spokes. In: Harris EH, Stern DB, Witman GB, editors. The Chlamydomonas Sourcebook (Second Edition). London: Academic Press. 209–234.
23. Mitchell DR (2009) Chapter 8 - The Flagellar Central Pair Apparatus. In: Harris EH, Stern DB, Witman GB, editors. The Chlamydomonas Sourcebook (Second Edition). London: Academic Press. 235–252.
24. Witman GB, Plummer J, Sander G (1978) Chlamydomonas flagellar mutants lacking radial spokes and central tubules. Structure, composition, and function of specific axonemal components. The Journal of cell biology 76: 729–747.
25. Lechtreck KF, Delmotte P, Robinson ML, Sanderson MJ, Witman GB (2008) Mutations in Hydin impair ciliary motility in mice. The Journal of cell biology 180: 633–643.
26. Huang B, Ramanis Z, Luck DJ (1982) Suppressor mutations in Chlamydomonas reveal a regulatory mechanism for Flagellar function. Cell 28: 115–124.
27. Piperno G, Mead K, Shestak W (1992) The inner dynein arms I2 interact with a "dynein regulatory complex" in Chlamydomonas flagella. The Journal of cell biology 118: 1455–1463.
28. Omoto CK, Kung C (1979) The pair of central tubules rotates during ciliary beat in Paramecium. Nature 279: 532–534.
29. Oda T, Yanagisawa H, Yagi T, Kikkawa M (2014) Mechanosignaling between central apparatus and radial spokes controls axonemal dynein activity. The Journal of cell biology 204: 807–819.
30. Nakazawa Y, Hiraki M, Kamiya R, Hirono M (2007) SAS-6 is a cartwheel protein that establishes the 9-fold symmetry of the centriole. Current biology: CB 17: 2169–2174.
31. Gibbons IR, Grimstone AV (1960) On flagellar structure in certain flagellates. The Journal of biophysical and biochemical cytology 7: 697–716.
32. Cavalier-Smith T (1974) Basal body and flagellar development during the vegetative cell cycle and the sexual cycle of Chlamydomonas reinhardii. Journal of cell science 16: 529–556.
33. Kitagawa D, Vakonakis I, Olieric N, Hilbert M, Keller D, et al. (2011) Structural basis of the 9-fold symmetry of centrioles. Cell 144: 364–375.
34. van Breugel M, Hirono M, Andreeva A, Yanagisawa HA, Yamaguchi S, et al. (2011) Structures of SAS-6 suggest its organization in centrioles. Science (New York, NY) 331: 1196–1199.
35. Mitchell DR, Sale WS (1999) Characterization of a Chlamydomonas insertional mutant that disrupts flagellar central pair microtubule-associated structures. The Journal of cell biology 144: 293–304.
36. Dutcher SK (1995) Mating and tetrad analysis in Chlamydomonas reinhardtii. Methods in cell biology 47: 531–540.
37. Gorman DS, Levine RP (1965) Cytochrome f and plastocyanin: their sequence in the photosynthetic electron transport chain of Chlamydomonas reinhardi. Proceedings of the National Academy of Sciences of the United States of America 54: 1665–1669.
38. Witman GB (1986) [28] Isolation of Chlamydomonas flagella and flagellar axonemes. In: Richard BV, editor. Methods in enzymology: Academic Press. 280–290.
39. Piperno G, Huang B, Luck DJ (1977) Two-dimensional analysis of flagellar proteins from wild-type and paralyzed mutants of Chlamydomonas reinhardtii. Proceedings of the National Academy of Sciences of the United States of America 74: 1600–1604.
40. Kamiya R (1982) Extrusion and Rotation of the central-pair microtubules in detergent-treated Chlamydomonas flagella. Progress in clinical and biological research 80: 169–173.
41. Mitchell DR, Nakatsugawa M (2004) Bend propagation drives central pair rotation in Chlamydomonas reinhardtii flagella. The Journal of cell biology 166: 709–715.
42. Dutcher SK, Huang B, Luck DJ (1984) Genetic dissection of the central pair microtubules of the flagella of Chlamydomonas reinhardtii. The Journal of cell biology 98: 229–236.
43. Feistel K, Blum M (2006) Three types of cilia including a novel 9+4 axoneme on the notochordal plate of the rabbit embryo. Developmental dynamics: an official publication of the American Association of Anatomists 235: 3348–3358.
44. Habermacher G, Sale WS (1995) Regulation of dynein-driven microtubule sliding by an axonemal kinase and phosphatase in Chlamydomonas flagella. Cell motility and the cytoskeleton 32: 106–109.
45. Yang P, Sale WS (2000) Casein kinase I is anchored on axonemal doublet microtubules and regulates flagellar dynein phosphorylation and activity. The Journal of biological chemistry 275: 18905–18912.
46. Smith EF (2002) Regulation of flagellar dynein by the axonemal central apparatus. Cell motility and the cytoskeleton 52: 33–42.
47. Warner FD, Satir P (1974) The structural basis of ciliary bend formation. Radial spoke positional changes accompanying microtubule sliding. The Journal of cell biology 63: 35–63.
48. Lindemann CB, Kanous KS (1995) "Geometric clutch" hypothesis of axonemal function: key issues and testable predictions. Cell motility and the cytoskeleton 31: 1–8.
49. Tamm SL, Tamm S (1981) Ciliary reversal without rotation of axonemal structures in ctenophore comb plates. The Journal of cell biology 89: 495–509.
50. Gadelha C, Wickstead B, McKean PG, Gull K (2006) Basal body and flagellum mutants reveal a rotational constraint of the central pair microtubules in the axonemes of trypanosomes. Journal of cell science 119: 2405–2413.
51. Gibbons IR (1961) The relationship between the fine structure and direction of beat in gill cilia of a lamellibranch mollusc. The Journal of biophysical and biochemical cytology 11: 179–205.
52. Yoshimura M, Shingyoji C (1999) Effects of the central pair apparatus on microtubule sliding velocity in sea urchin sperm flagella. Cell structure and function 24: 43–54.

53. Brown JM, Dipetrillo CG, Smith EF, Witman GB (2012) A FAP46 mutant provides new insights into the function and assembly of the C1d complex of the ciliary central apparatus. Journal of cell science 125: 3904–3913.

54. Smith EF (2002) Regulation of flagellar dynein by calcium and a role for an axonemal calmodulin and calmodulin-dependent kinase. Molecular biology of the cell 13: 3303–3313.

55. Wargo MJ, Smith EF (2003) Asymmetry of the central apparatus defines the location of active microtubule sliding in *Chlamydomonas* flagella. Proceedings of the National Academy of Sciences of the United States of America 100: 137–142.

56. Randall J, Warr JR, Hopkins JM, McVittie A (1964) A SINGLE-GENE MUTATION OF *CHLAMYDOMONAS REINHARDII* AFFECTING MOTILITY: A GENETIC AND ELECTRON MICROSCOPE STUDY. Nature 203: 912–914.

57. Randall JT, Cavalier-Smith T, McVittie A, Warr JR, Hopkins JM (1967) Developmental and control processes in the basal bodies and flagella of *Chlamydomonas reinhardtii*. Dev Biol suppl 1: 43–83.

58. Warr JR, McVittie A, Randall JT, Hopkins JM (1966) Genetic control of flagellar structure in *Chlamydomonas reinhardtii*. Genet Res 7: 335–351.